Korean J. Chem. Eng., 33(10), 3016-3020 (2016)
DOI: 10.1007/s11814-016-0173-8

pISSN: 0256-1115
eISSN: 1975-7220

Combustion of boron particles coated with an energetic polymer material

Weon Gyu Shin*, Doohee Han, Yohan Park***, Hyung Soo Hyun****, Hong-Gye Sung**,†, and Youngku Sohn***,†**

*Department of Mechanical Engineering, Chungnam National University, Daejeon 34134, Korea
**School of Aerospace and Mechanical Engineering, Korea Aerospace University, Goyang, Gyeonggi-do 21071, Korea
***Department of Chemistry, Yeungnam University, Gyeongsan, Gyeongbuk 38541, Korea
****The Fourth R&D Institute, Agency for Defense Development, Daejeon 34188, Korea
(*Received 15 March 2016 • accepted 20 June 2016*)

Abstract−Elemental boron has attracted considerable attention as a potential high energetic material for explosives and propellants. However, its use has been hindered by its high vaporization temperature and surface oxide layer. In this study, boron particles were coated with glycidyl azide polymer (GAP) to improve their combustion characteristics. The coated particles were characterized by transmission electron microscopy, X-ray photoelectron spectroscopy (XPS) and Fourier-transform infrared spectroscopy. XPS performed before and after Ar+ ion sputtering confirmed that the azide ($-N_3$) group of GAP was positioned at the proximity of the boron surface. In addition, B@GAP particles could be decorated with metallic Ag (~10 nm) nanoparticles. The combustion characteristics were examined using a newly designed pre-heated (1,800 K) drop tube furnace and a high speed camera. Two stages of combustion were observed for a dust cloud of GAP-coated boron particles. The burning time was estimated to be approximately 37.5 msec.

Keywords: Boron, Glycidyl Azide Polymer, Drop Tube Furnace, Combustion, Burning Time

INTRODUCTION

Boron (B) with a low atomic mass (10.8 g/mol) has potential applications as an energetic material for explosives and propellants because of its very high gravimetric (58 kJ/g) and volumetric (136 kJ/cm^3) heat of combustion [1-3]. However, it has not been used efficiently as a high energy release material because of its disadvantages, such as the protective boron oxide layer and high vaporization temperature (~2,530 °C) [4-6]. The ignition delay time increases with increasing initial oxide layer thickness [3]. Considerable efforts have been devoted to removing the oxide layer, better understanding the ignition of elemental boron [1,5] and enhancing combustion using composite materials. Such composites include Ti-B, B-Mg, LiF-B, silane-B, B-Li, B-Al, and metal oxide-B [2,11-15]. Hu et al. reported ignition times of 4 and 22 msec for 5 and 20 mm boron particles (with an initial oxide layer of 0.1 mm), respectively, at an ambient gas temperature of 2,050 K [1]. The ignition time increased monotonically with increasing particle size, which was attributed to an increase in the mass-to-surface ratio. Xi et al. reported that the boron oxide (B_2O_3) layer could be removed by oxalic acid. Therefore, the ignition delay time and combustion intensity were decreased by 42.4% and 16.7%, respectively [5]. For Ti addition to boron, the exothermic intermetallic reaction ($Ti+2B \rightarrow TiB_2$, $\Delta H=-4.02$ kJ/g) could enhance boron ignition and combustion [2,13,14]. Trunov et al. reported that the burn rates and combustion energy of the Ti-2B nanocomposite powder were higher than those of Al in all $N_2/O_2/CH_4$ mixture environments [2]. Coating boron with an energetic polymer has also been shown to enhance the ignition of boron [9,16]. Oleic acid has been used to prevent boron oxidation during ball milling [19,17]. The polymer coating prevents boron from forming an oxide layer. The additional high energy from the polymer can also be utilized. Glycidyl azide polymer (GAP) is a well-known energetic polymer with a low glass-transition temperature [18-23]. Because the polymer contains an azide group ($-N_3$) during decomposition, it releases very high energy ($\Delta H=-485$ cal/g) [24], which facilitates the ignition of boron. Lima et al. produced butyloxy-functionalized boron particles and added GAP to enhance the combustion of boron particles [3].

Previously, Shyu and Liu examined the ignition and combustion of GAP-coated boron particles. Their experimental conditions, however, were very different from those in the present study (ambient gas environment, atmospheric pressure, and preheated tube furnace at 1,800 K). They injected the particles into a hot (2,343 K) gaseous environment generated from a flat-flame burner using premixed (propane-oxygen-nitrogen) gases. Therefore, this study has novelty in that the ignition and combustion data were obtained under different experimental conditions of a lower temperature and ambient gas environment. A metal coating on a material has been used to alter the physicochemical properties. A range of coating methods have been introduced, including vapor deposition, wet (photo-irradiation) solution method, thermal spray coating, and electrospinning method [25-27]. Metallic Ag nanoparticles (NPs) have commonly been deposited by a photo-irradiation method in solution [27]. This method was used in the present study to deposit Ag NPs on the GAP-coated boron particles.

In the present work, boron particles were coated efficiently with

†To whom correspondence should be addressed.
E-mail: youngkusohn@ynu.ac.kr, hgsung@kau.ac.kr

GAP using a facile solution process. The combustion characteristics (e.g., burning time) of the GAP-coated boron particles were examined using a preheated drop tube furnace, where dust cloud state particles were dropped inside the furnace and captured by a high speed camera during ignition and combustion. The technology of using a high speed camera in this study is more advanced than that reported 20 years ago [16]. The novelty also includes a live color image of high speed burning particles in the vertical furnace that provides direct evidence of a second-stage of combustion of boron particles. This study provides new insights into the improvement of boron combustion by demonstrating a high energy polymer coating and measuring the burning time.

EXPERIMENTAL

1. Materials

For the GAP coating on the boron particles, GAP was dissolved in dimethyl formamide (DMF). GAP (MW=2400, HEPCE CHEM Co., Ltd., South Korea) was used as received. Boron powder (Yingkou Tanyun Chemical Research Institute Co. Ltd., average size of 30 μm, 95%) was dispersed in the GAP solution with sonication. The GAP/B weight ratio was 0.01-0.2, which corresponds to 1-20 wt% GAP. Upon sonication for 10 min, isopropyl alcohol (IPA) was added slowly to the boron-GAP solution. During addition, the GAP-coated boron particles precipitated. The resulting precipitates (B@GAP) were filtered and finally dried in a vacuum oven at 50 °C. For the Ag coating on B@GAP material, the material was dispersed in an Ag nitrate solution (0.01 M) and irradiated with UV for 1 hour to obtain the Ag nanoparticles. The solution was then centrifuged to collect the powder. The product (B@GAP-Ag) was dried in a vacuum oven at 50 °C.

2. Characterization

The B@GAP and B@GAP-Ag were placed on a Cu grid and the morphologies were examined by transmission electron microscopy (TEM, Hitachi H-7600) at an operation voltage of 100 keV. Fourier transform infrared (FT-IR, Thermo Scientific Nicolet iS10) spectroscopy was performed in attenuated total reflectance (ATR) mode. X-ray photoelectron spectroscopy (XPS, MultiLab 2000 Thermo Scientific, USA) was conducted using monochromatic AlKα X-rays. XPS was also performed after Ar^+ ion sputtering for 60 sec using a 3 kV and 1 μA beam.

3. Combustion Test

To examine the combustion characteristics, the B@GAP particles were dropped into a tube furnace. A dust cloud state of GAP-coated boron particles was formed by air-pressurized injection into the high temperature tube furnace, which was preset to a temperature of 1,800 K. A schematic of the experimental setting will be described later.

RESULTS AND DISCUSSION

Fig. 1 details the procedure for the GAP-coating on the boron particles. GAP is soluble in organic solvents, such as DMF and dimethyl sulfoxide (DMSO), but it is insoluble in IPA and water [16]. A pair of solvents (DMF and IPA) were chosen: one for dissolving GAP and the other for precipitating the GAP on boron.

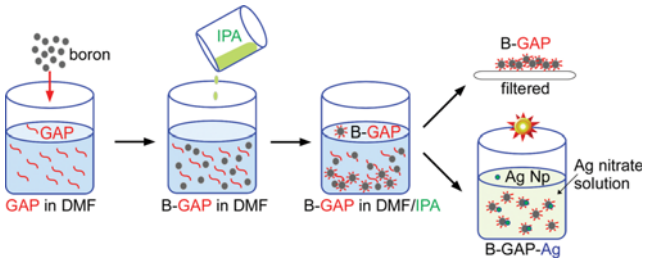

Fig. 1. Schematic diagram of the coating procedures.

Boron particles are insoluble, but can be well dispersed in both solvents. Boron particles were first dispersed fully in the GAP-dissolved DMF solution. When IPA was added slowly to the boron-dispersed solution, GAP precipitated on the boron particles because of its insolubility in IPA. An IPA/DMF volume ratio of 10/1 was used to obtain the complete precipitation of GAP. Because GAP is a sticky material, the GAP on boron resulted in aggregation in the solution and settling on the bottom of a beaker. The GAP coating was detected easily by the naked eye. Once the precipitates were fully settled, the GAP-coated boron (B@GAP) was filtered to separate the solvents. The Ag decoration on the B-GAP material was accomplished using an Ag^+ ion reduction method under UV light. The B@GAP particles were first dispersed in a 0.01 M Ag nitrate solution and placed under UV light for 1 hour. The particles were collected again by centrifugation.

Fig. 2 presents TEM images of the GAP-coated boron (B@GAP) and Ag-decorated GAP-coated boron (B@GAP-Ag) particles. The TEM images confirmed the coating of GAP and Ag decoration. For the B@GAP, the surface was damaged (or melted) during the TEM observations. The TEM image shows many tiny holes on the surface. Therefore, it was concluded that GAP is damaged easily by the electron beam. The surface of boron particles was also coated uniformly by GAP. For B@GAP-Ag, the surface showed no electron beam damage, unlike B@GAP. This suggests that the chemical structure of soft GAP was changed to a hard material. Because GAP contains a reactive azide ($-N_3$) group as the major functional group [18-20], the functional group can react chemically to form another structure. The spherical shapes were attributed to Ag nanoparticles (NPs), approximately 10 nm in size. A photo-reduction method is used widely to deposit precious metals, such as Ag, Au, and Pt [27]. No post-treatment is required to remove the

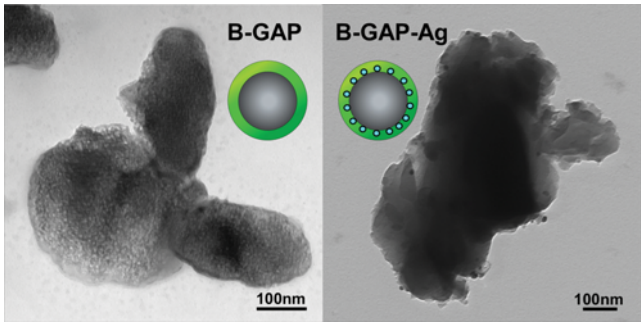

Fig. 2. TEM images of GAP-coated boron (B@GAP) and Ag-decorated GAP-coated boron (B@GAP-Ag) particles.

residual reductant because no reductant is used in this method. For Ag NP deposition, the reduction occurs via $Ag^{+}+H_2O \rightarrow Ag^{0}+H^{+}+\cdot OH$ [27].

FT-IR spectroscopy is an important tool for identifying the $-N_3$ group of GAP [20,23,41]. Fig. 3 presents the FT-IR spectra of bare and GAP-coated (2, 5, 10, and 20 wt%) boron particles. The inset shows the chemical structure of GAP. The FT-IR spectrum of bare boron showed no characteristic peak. On the other hand, for the B@GAP material, a new absorption peak appeared at ~2,100 cm^{-1}, which was attributed to the asymmetric stretching band of $-N_3$ [18,22,42]. The intensity of the fingerprint IR peak increased with increasing amount of GAP material. No OH vibration peak was observed at approximately 3,200 cm^{-1}.

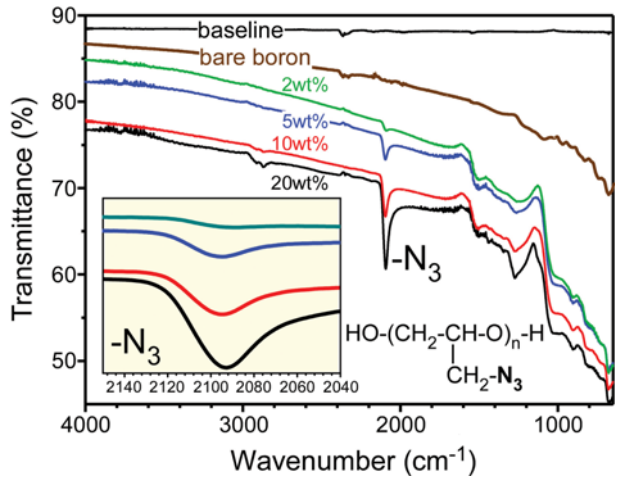

Fig. 3. FT-IR spectra of bare and GAP-coated (2, 5, 10, and 20 wt%) boron particles. The inset shows the chemical structure of GAP and the expanded stretching band of $-N_3$.

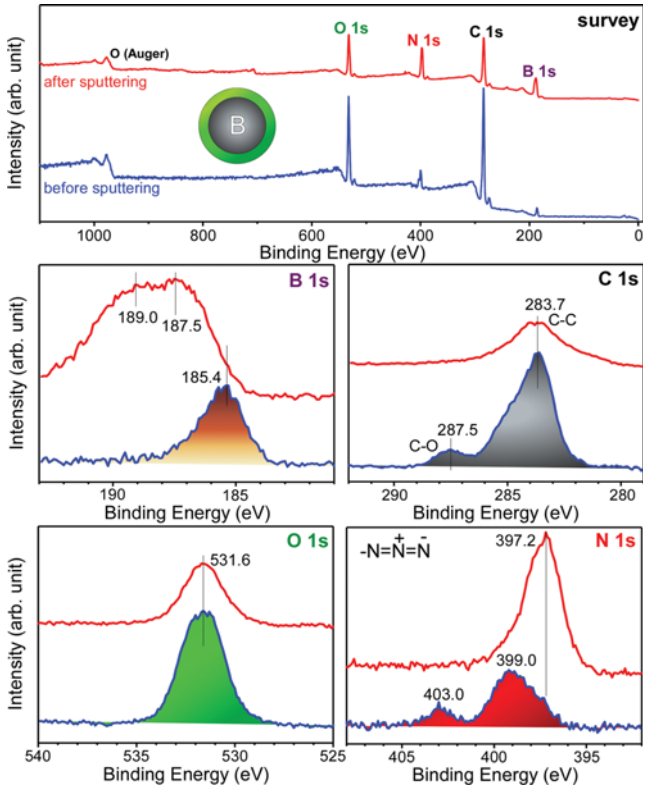

Fig. 4. Survey and high-resolution (B 1s, C 1s, O 1s, and N 1s) XPS spectra of B@GAP sample.

Fig. 4 shows the survey and high resolution B 1s, C 1s, O 1s, and N 1s XP spectra of the GAP-coated boron (B@GAP) particles before and after Ar^{+} ion sputtering. The survey scan reveals carbon, oxygen, and nitrogen for the GAP material, and boron. The B 1s XP spectrum before sputtering shows a peak at 185.4 eV, which is 2.1 eV lower than that (187.9 eV) observed for bare boron [43]. The lower BE can be attributed to an electron donating group near the boron surface. For GAP on boron, the $-N_3$ group of GAP is an electron donating group that is positioned plausibly on the proximity of the electron deficient boron surface, forming B-N_3-R. For the C 1s XPS peaks, two peaks are observed at 283.7 eV (major) and 287.5 eV (minor), which were assigned to C-C and C-O species of the outer layer of the GAP material. The weak shoulder peak between the two C 1s peaks is attributed to the C-N species of GAP. A broad O 1s peak at 531.6 eV was attributed to the O-C species of GAP. N 1s XPS reveals two peaks at 399.0 (major) and 403.0 eV (minor), which were assigned to the electron-rich and -deficient nitrogen atoms of the azide group. This is in good agreement with the literature [41]. For the aryl-azide-terminated self-assembled monolayers on the Au substrates, two N 1s peaks were observed at 400.5 (major) and 403.8 eV (minor) with an intensity ratio of 2 [41].

Several changes were observed in the survey and high resolution XP spectra taken after Ar^{+} ion sputtering. The intensity of the B 1s XP spectrum increased dramatically and the peak positions (187.5 and 189.0 eV) were clearly different from that (185.4 eV) before sputtering. The increase in the B 1s XPS peak was attributed to the removal of the outer layer GAP material by Ar^{+} ion sputtering. The new B 1s peak at 187.5 eV was assigned to elemental boron exposed after sputtering [17]. The B 1s peak at 189.0 eV was assigned to B-N species formed during sputtering [44]. B-O species were excluded because the BE is generally located at a much higher position [17,43,44]. The formation of B-N like species by the Ar^{+} ion sputtering beam is plausible because the $-N_3$ group is positioned near the boron surface before sputtering. The N 1s XPS peak was also changed significantly and observed at 397.2 eV with increasing intensity. The new N 1s XPS peak suggests that the chemical state of N was changed dramatically by sputtering. The new N 1s XPS peak was assigned to N-B. As mentioned above, the carbon and oxygen of GAP are positioned outside, whereas the N of GAP is located deep inside. The outside C and O are removed by sputtering. Therefore, the inside N is more exposed to the surface. As a consequence, the C 1s and O1s XPS peaks decrease with a concomitant increase in the N 1s XPS peak, as observed in the present XPS results.

Fig. 5 shows the survey and high-resolution Ag 3d, B 1s, C 1s, O 1s, and N 1s XP spectra of the as-prepared B@GAP-Ag sample. The survey scan showed peaks corresponding to Ag, B, C, O, and N. For the Ag 3d XPS spectrum, two Ag $3d_{5/2}$ (Ag $3d_{3/2}$) XPS peaks were observed at 368.3 (374.3) eV with a spin-orbit coupling of 6.0 eV. These peaks were assigned to the decorated metallic Ag

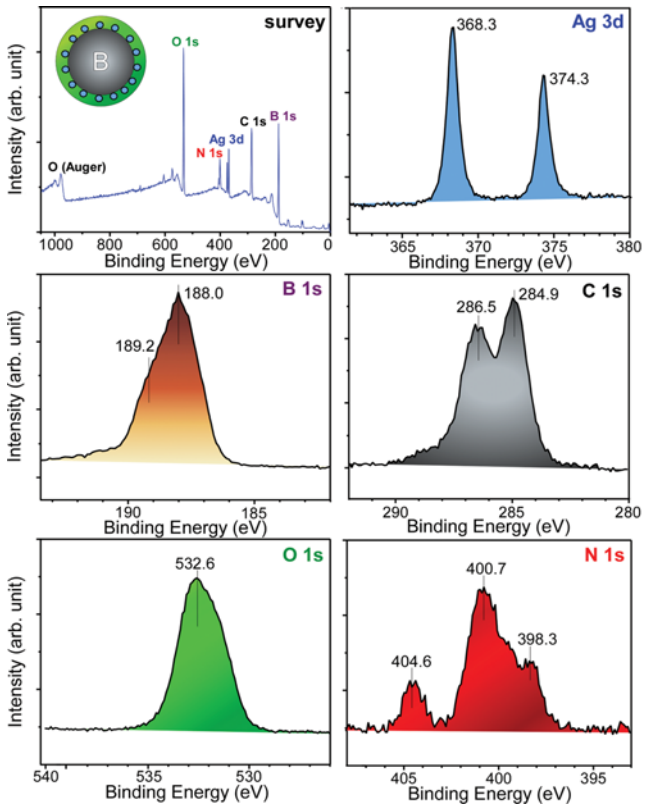

Fig. 5. Survey and high-resolution (Ag 3d, B 1s, C 1s, O 1s, and N 1s) XP spectra of the B@GAP-Ag sample.

NPs [45,46]. The maximum of the B 1s XPS peak was located at 188.0 eV with a very weak shoulder peak at 189.2 eV. The B 1s peak is very close to a BE of 187.9 eV for bare boron [43]. The C 1s, O 1s, and N 1s XPS peaks for the B@GAP-Ag material were significantly different from those of the B@GAP material. This suggests that the chemical state of GAP changed dramatically upon Ag decoration under UV irradiation. An asymmetric broad O 1s XPS peak was observed at 532.6 eV, which was 1.0 eV higher than that found for the B@GAP material. Two strong C 1s XPS peaks were noted at 284.9 and 286.5 eV. The N 1s XPS peaks were observed at 398.3, 400.7, and 404.6 eV. The spectrum of this material shows a new N 1s peak at 398.3 compared to that of the B@GAP material. When GAP is irradiated with light (or heat is applied), it is expected to form N=C species [6]. Radhakrishnan et al. reported a similar N 1s XPS result for an azide with CdS quantum dots after photocatalytic reduction [41].

Fig. 6 presents a schematic diagram of the experimental apparatus to measure the burn time of the dropping dust cloud using a vertical preheated furnace. The inside was heated to 1,800 K (1,527 °C) to ignite the dropping particles. The temperature was high enough to ignite the B@GAP particles because the ignition temperature of boron (2.5-13.4 mm) is 1,350-1,480 °C in air [15]. The particles were injected at the top of the furnace using compressed air to allow dust particles to be dispersed. Otherwise, the GAP-coated boron particles tend to form aggregates because the GAP is a viscous material. The luminous dropping (by gravity) of particles was observed through the quartz windows and their motions and burning behaviors were tracked (or imaged) using a high speed camera. The camera can take more than 2000 image frames per second (FPS), i.e., the time between the two neighboring images (or frames) was 0.5 msec. Therefore, the high speed camera can track the burning of each clustered particle directly. This design could provide more useful information for understanding the combustion of an energetic material.

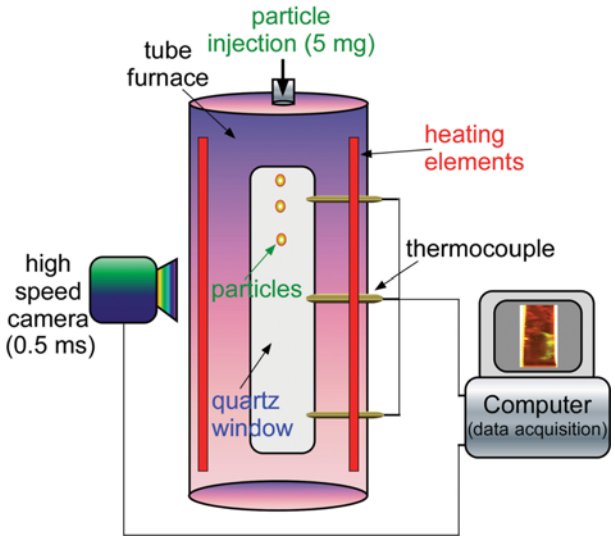

Fig. 6. Schematic diagram of the burn time measurement apparatus of the cloud particles.

Fig. 7 displays the selected images taken using a high speed camera (2000 FPS) when the particles were dropping. A movie containing all image frames is provided in the Supporting Information. A 5 mg sample of B@GAP particles was injected by compressed air to form a well distributed dust cloud. The first two images show

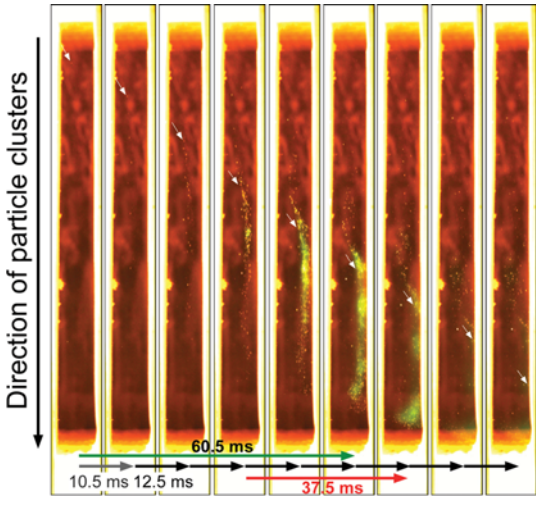

Fig. 7. Selected images of the ignition of vertically dropping B@GAP particles. The time interval between the first and second frames was 10.5 msec, and others between the neighboring frames were 12.5 msec. The arrows track the movement of a single particle.

the particles in the preheated state. The particles ignite and burn continuously. At least two colors are observed through the image: yellow and green. This suggests that the second-stage combustion of boron had taken place [15]. The yellow color indicates ignition and the first-stage combustion of boron, and the green was attributed to BO_2 emission [4,5]. BO_2 is a reactive intermediary gas molecule formed during boron ignition [4]. The spectrum of BO_2 emission was observed at 492, 518, and 545 nm, corresponding to a green color region [4]. The green color appeared after 37.5 msec from the first image frame and became strongest after 60.5 msec. Combustion decreased after intense green emission. The burn time of the B@GAP particle was estimated to be approximately 37.5 msec. Shyu and Liu also prepared GAP (MW≈2000)-coated boron (~50 mm) particles, and examined the combustion residues and the ignition/combustion time under hot gaseous environments. The hot environment (~2,343 K) was achieved using a flat-flame burner with premixed propane-O_2-N_2 gases [16]. They reported that the GAP-coated boron showed a shorter ignition delay time and combustion time than bare boron [16]. They also reported total burning times of 52.7 msec and 39.0 msec for bare boron and GAP-coated (9.2%) boron, respectively, under 6.49% O_2 excess conditions. The burn times decreased to 47.1 msec and 31.5 msec, respectively, under a 23.79% O_2 excess. These values were in good agreement with the present results.

CONCLUSIONS

Boron particles were coated efficiently with GAP by a wet solution process to enhance the combustion characteristics of boron. B@GAP was also decorated with Ag NPs. A uniform GAP coating, and the presence of -N_3 groups was confirmed by TEM and FT-IR spectroscopy, respectively. XPS performed before and after Ar^+ ion sputtering showed that the -N_3 group was positioned at the proximity of the boron surface. Energy transfer to boron appeared to be more efficient at the proximity position. This position may help further enhance the combustion of boron. Using a newly designed pre-heated drop tube furnace and a high speed camera (2000 FPS), it was found that the dust cloud GAP-coated boron had two stages of combustion with a total burn time of approximately 37.5 msec. Overall, this study provides new insights into the development of high energetic materials and a combustion study setup.

ACKNOWLEDGEMENT

This study was supported financially by ADD-12-01-04-05. The authors acknowledge the HEPCE CHEM Co., Ltd. for providing GAP.

SUPPORTING INFORMATION

Additional information as noted in the text. This information is available via the Internet at http://www.springer.com/chemistry/journal/11814.

REFERENCES

1. J. X. Hu, Z. X. Xia, W. H. Zhang, Z. B. Fang, D. Q. Wang and L. Y. Huang, *Int. J. Aerospace Eng*., **2012**, 160620 (2012).
2. M. Trunov, V. Hoffmann, M. Schoenitz and E. L. Dreizin, *J. Propul. Power*, **24**, 184 (2008).
3. R. J. P. Lima, C. Dubois, O. Mader, R. Stowe and S. Ringuette, *Int. J. Energetic Mater. Chem. Prop*., **9**, 437 (2010).
4. R. O. Foelsche, R. L. Burton and H. Krier, *Combust. Flame*, **117**, 32 (1999).
5. J. Xi, J. Liu, Y. Wang, D. Liang, H. Li and J. Zhou, *Propellants Explos. Pyrotech*., **39**, 844 (2014).
6. C.-J. Tang, Y. J. Lee and T. A. Litzinger, *Combust. Flame*, **117**, 244 (1999).
7. S. Mohan, M. A. Trunov and E. L. Dreizin, *J. Propul. Power*, **24**, 199 (2008).
8. B. Van Devener, J. P. L. Perez, J. Jankovich and S. L. Anderson, *Energy Fuels*, **23**, 6111 (2009).
9. D. Meinköhn, *Combust. Sci. Technol*., **176**, 1493 (2004).
10. B. Hussmann and M. Pfitzner, *Combust. Flame*, **157**, 803 (2010).
11. J.-F. Xi, J.-Z. Liu and Y. Wang, *J. Solid Rocket Technol*., **36**, 654 (2013).
12. J.-Z. Liu, J.-F. Xi and W.-J. Yang, *Acta Astronaut*., **96**, 89 (2014).
13. M. D. Clemenson, S. Johnson, H. Krier and N. Glumac, *Propellants Explos. Pyrotech*., **39**, 454 (2014).
14. X. Jiang, M. Trunov, M. Schoenitz, R. Dave and E. L. Dreizin, *J. Alloys Compd*., **478**, 246 (2009).
15. C. L. Yeh and K. K. Kuo, *Prog. Energy Combust. Sci.*, **22**, 511 (1996).
16. I. M. Shyu and T. K. Liu, *Combust. Flame*, **100**, 634 (1995).
17. B. V. Devener, J. P. L. Perez and S. L. Anderson, *J. Mater. Res*., **24**, 3462 (2009).
18. C. Hu, X. Guo, Y. Jing, J. Chen, C. Zhang and J. Huang, *J. Appl. Polym. Sci*., **131**, 40636 (2014).
19. B. S. Min, Y. C. Park and J. C. Yoo, *Propellants Explos. Pyrotech*., **37**, 59 (2012).
20. B. S. Min and S. W. Ko, *Macromol. Res*., **15**, 225 (2007).
21. S. Brochu and G. Ampleman, *Macromolecules*, **29**, 5539 (1996).
22. J.-S. You, J.-O. Kweon, S.-C. Kang and S.-T. Noh, *Macromol. Res*., **18**, 1226 (2000).
23. T. Wang, S. Li, B. Yang, C. Huang and Y. Li, *J. Phys. Chem. B*, **111**, 2449 (2007).
24. K. Selim, S. Ozkar and L. Yilmaz, *J. Appl. Polym. Sci*., **77**, 538 (2000).
25. G. Xanthopoulou, A. Marinou, G. Vekinis, A. Lekatou and M. Vardavoulias, *Coatings*, **4**, 231 (2014).
26. F. Iskandar, *Adv. Powder Technol*., **20**, 283 (2009).
27. M. Sakamoto, M. Fujistuka and T. Majima, *J. Photochem. Photobiol. C*, **10**, 33 (2009).
28. C. Radhakrishnan, M. K. F. Lo, M. V. Warrier, M. A. Garcia-Garibay and H. G. Monbouquette, *Langmuir*, **22**, 5018 (2006).
29. Y. Sun and S. Li, *J. Hazard. Mater*., **154**, 112 (2008).
30. W. G. Shin, H. J. Jung, H. G. Sung, H. S. Hyun and Y. Sohn, *Ceram. Inter*., **40**, 11511 (2014).
31. S. Wan, Y. Yu, J. Pu and Z. Lu, *RSC Adv*., **5**, 19236 (2015).
32. Y. Sohn, *J. Mol. Catal. A*, **379**, 59 (2013).
33. J. G. Kang and Y. Sohn, *J. Mater. Sci*., **47**, 824 (2012).